

*Invited Paper*

## Nanoporous Platforms for Cellular Sensing and Delivery

Lara Leoni<sup>1</sup>, Darlene Attiah<sup>1</sup> and Tejal A. Desai<sup>1,2,\*</sup>

<sup>1</sup>Department of Bioengineering, University of Illinois at Chicago; <sup>2</sup>Department of Biomedical Engineering, Boston University, 44 Cummington Street, Boston, MA 02215, USA. Tel: (617) 358-3054. Fax: (617) 353-6766.

\* Author to whom correspondence should be addressed. E-mail: [tdesai@bu.edu](mailto:tdesai@bu.edu)

Received: 5 March 2002 / Accepted: 19 March 2002 / Published: 20 March 2002

---

**Abstract:** In recent years, rapid advancements have been made in the biomedical applications of micro and nanotechnology. While the focus of such technology has primarily been on in vitro analytical and diagnostic tools, more recently, in vivo therapeutic and sensing applications have gained attention. This paper describes the creation of monodisperse nanoporous, biocompatible, silicon membranes as a platform for the delivery of cells. Studies described herein focus on the interaction of silicon based substrates with cells of interest in terms of viability, proliferation, and functionality. Such microfabricated nanoporous membranes can be used both in vitro for cell-based assays and in vivo for immunoisolation and drug delivery applications.

**Keywords:** Nanotechnology, Drug delivery, Silicon, Immunoisolation, Cell-based assays.

---

### Introduction

The application of micro- and nanotechnology to the biomedical arena has tremendous potential in terms of developing new diagnostic and therapeutic modalities and has increasingly been used to solve complex problems at the molecular and cellular level. While the majority of research has focused on the development of miniaturized *diagnostic* tools such as electrophoretic, chromatographic, and cell micromanipulation systems [1-5], researchers have more recently concentrated on the development of microdevices and constructs for *therapeutic* applications. Micro- and nanofabrication techniques are currently being used to develop implants that can record from, sense, stimulate, and deliver to biological systems. Micromachined neural prostheses, drug delivery micropumps/needles, and microfabricated immunoisolation biocapsules [6-9] have all been fabricated using precision-based

microtechnologies. Microfabrication methods have also been applied to biotechnology in areas such as DNA sequencing by hybridization, protein patterning, and functional cell sorting.

The interfacing of "chip" technology and cell biology has great potential for use in biomedical research. Moreover, the human body seems appropriate as a target of microtechnology since most structures in the body are in the micron to millimeter size range, the same size range as most micro and nanoscale constructs. Few other engineering technologies can so closely parallel the multidimensional size scale of the living cells and tissues, with both precision and accuracy, in the same fabrication process. The miniaturization and reproducibility of platform features greatly facilitates the use of these systems for cell-based applications.

Microfabricated substrates can provide unique advantages over traditional biomaterials used for biosensing and delivery due to the: 1) ability to control surface microarchitecture, topography, and feature size in the nanometer and micron size scale, and 2) control of surface chemistry in a precise manner through biochemical coupling or photopatterning processes. Microfabrication technologies, by their very nature, lend themselves to efficient, economic mass-scale replication, as convincingly demonstrated by the microelectronic industry. They also allow for precise control of feature size, chemistry, and topography. The long term integration of cells with inorganic materials such as silicon provides the basis for novel delivery and sensing platforms. Our recent work has focused on the ability to maintain cells long term in nanoporous silicon-based microenvironments.

## Results and Discussion

Silicon nanoporous membranes were fabricated with pore sizes ranging from 7 nm to 49 nm as described in Leoni and Desai, 2001 [10]. The pore size was controlled through a sacrificial oxide etching which allows one to create nanoscale features using conventional lithography. Figure 1 shows the overall process flow of the membrane fabrication and is discussed in details in the experimental methods section. Figure 2 shows a cross sectional SEM image of the membrane with the nanoscale channels visible. The membranes can be fabricated in arrays on a single wafer, allowing one to produce multiple nanoporous membranes for *in vitro* or *in vivo* applications.

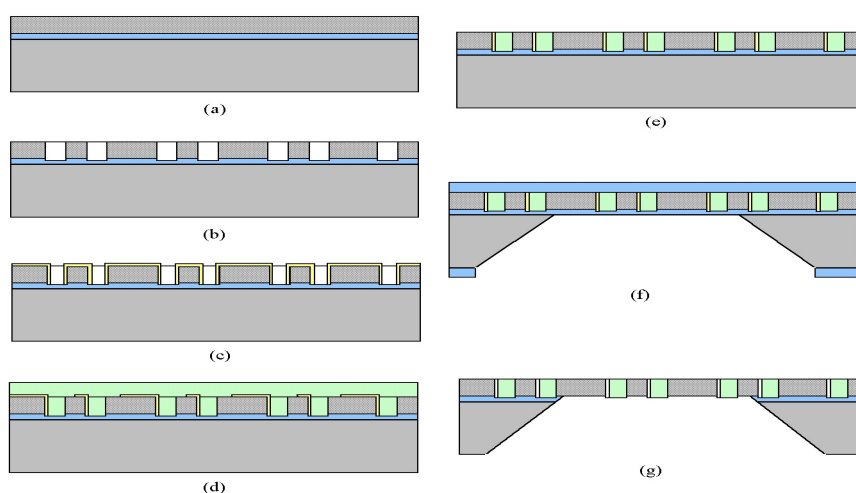


**Figure 1.** Process flow diagram for nanoporous membrane fabrication.

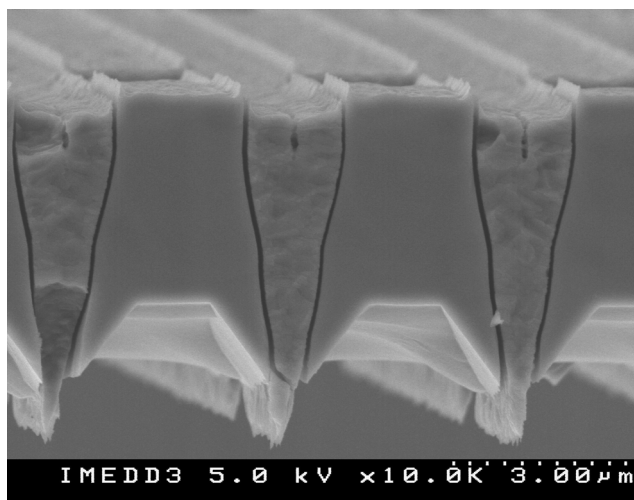


**Figure 2.** SEM micrograph of microfabricated nanoporous membrane: side view detail.

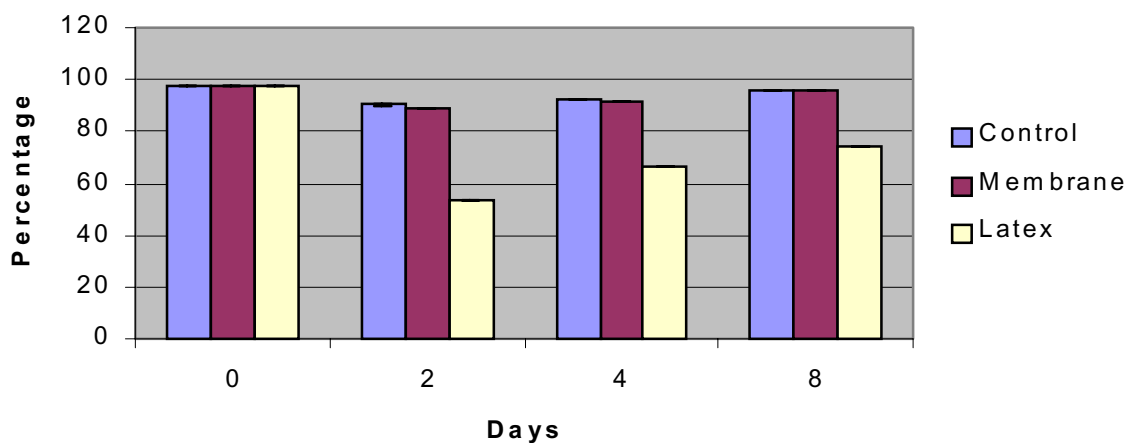


**Figure 3.** Viability of insulinoma cells over an 8-day period compared to control surface (petri dish) and negative control (latex).

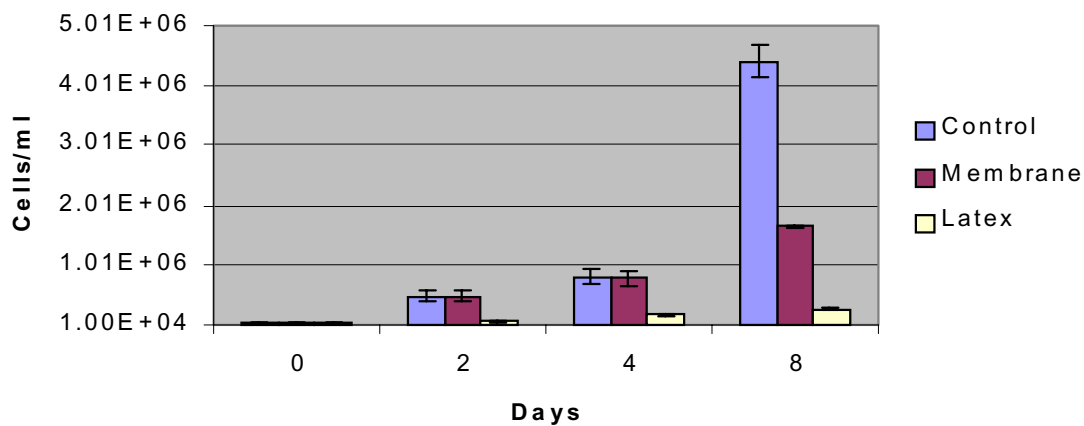


**Figure 4.** Proliferation of insulinoma cells over an 8-day period compared to control surface (petri dish) and negative control (latex).

### *Insulinoma Cells*

Silicon nanoporous membranes, control petri dishes, and latex membranes were seeded with insulinoma cells as described. We found that the insulinoma cells grew without any marked changes on the silicon surfaces. In fact, viability of the cells in the silicon nanoporous environments was equivalent to conventional cell culture surfaces, ranging from 100 to 90 percent over an eight day period (figure 3). All cell types had normal morphology. In terms of proliferation, cells seeded in nanoporous microenvironments had similar levels of proliferation compared to control surfaces up to day 4 and then a decreased rate of proliferation at day 8 (figure 4). This behavior was presumably due to contact inhibition resulting from the limited nanoporous surface area that cells were seeded in as compared to the control surface area. Cells exhibited limited viability and proliferation on the negative control surface of latex. Figure 5 shows an image of insulinoma cells growing on a partially etched nanoporous membrane. It is interesting to note that the cells limit their attachment to the porous regions of the membrane. Such behavior could be due to the nanopores providing a greater surface area for cells to attach. In addition, the etched porous surface is more hydrophilic as its final etch step is in HF solution and therefore may promote greater cell attachment. Figure 6 shows that cells insulinoma cells seeded in silicon nanoporous microenvironments are indeed functional and can secrete insulin over time. Glucose-supplemented medium was allowed to diffuse to the cells, through the membrane, to stimulate insulin production and monitor cell functionality. Results indicate that the insulin secretion by cells and subsequent diffusion of the insulin through the nanoporous membrane channels is similar to that of cell grown in culture.

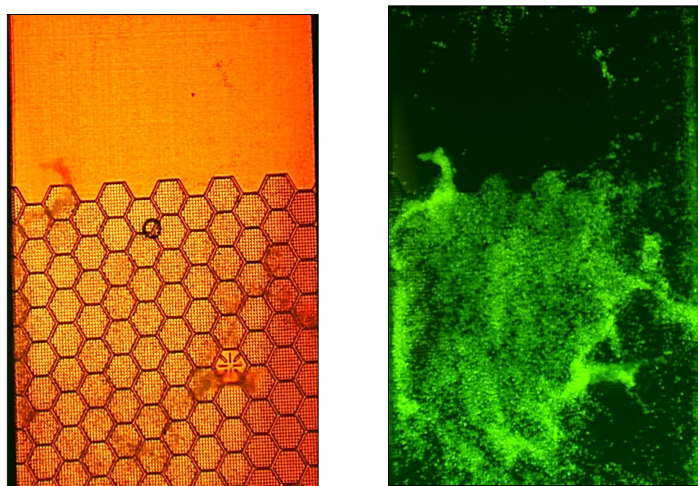


**Figure 5.** Micrograph of a) top surface of partially etched nanoporous membrane and b) nanoporous membrane seeded with fluorescently labeled insulinoma cells. Note the preferential adhesion of the cells to the etched membrane architecture.

### *Diffusion Properties*

When nutrients and time sensitive compounds are diffusing across a membrane, it is highly desirable to be able to precisely control the diffusion characteristics in order to retain the dynamic response of cells seeded on the membrane to external stimuli. The ability of the nanoporous

microfabricated membranes to perform size-base exclusion and controlled diffusion of biomolecules has been studied. Membranes exhibited controlled diffusion of glucose and albumin based on membrane pore size. Such control over molecular diffusion was precise and reproducible (figure 7).

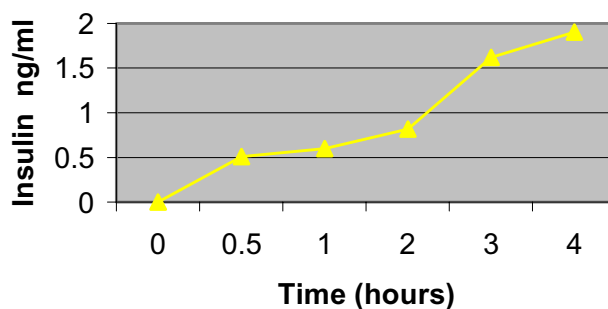


**Figure 6.** Insulin secretion profile from cells seeded on nanoporous membranes.

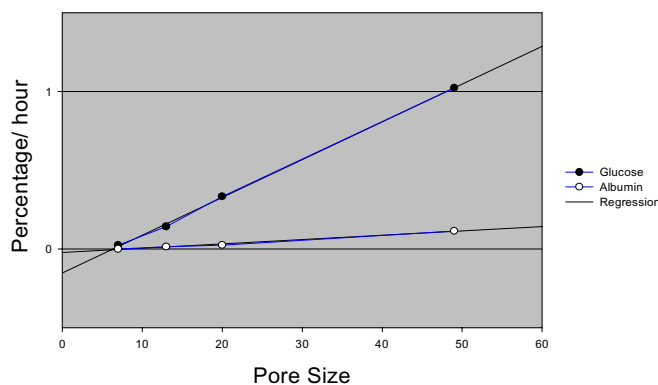


**Figure 7.** Glucose and Albumin diffusion rates.

### PC12 Cells

We found that PC12 cells also maintained approximately 100% viability as compared to control surfaces and actually proliferated to a greater extent in silicon nanoporous environments. Figure 8 shows empty nanoporous wells and wells seeded with PC12 cells at day 1 and day 7. The cells are able to become confluent and differentiated within the nanoporous wells. Cells seeded to the silicon nanoporous membranes experienced an approximate  $245.31\% \pm 62.5\%$  growth increase from day 1 to day 4 while those seeded to the polyurethane (control) capsules encountered only a  $75.9\% \pm 21\%$  growth increase (Figure 9). Moreover, cells attached to the silicon nanoporous membranes underwent high proliferation, increasing in number by approximately two fold every other day of the culture period. At day 1 of cell culture, the number of cells attached to the silicon based biocapsules and control capsules were observed approximately equal. By day 4, however, the silicon biocapsules exhibited a  $110\% \pm 35.36\%$  greater number of adherent cells. In contrast to the polyurethane capsules,

cells that were attached to the silicon biocapsules were noticed to attach firmly to the membrane as they strongly resisted detachment upon trypsinizing.

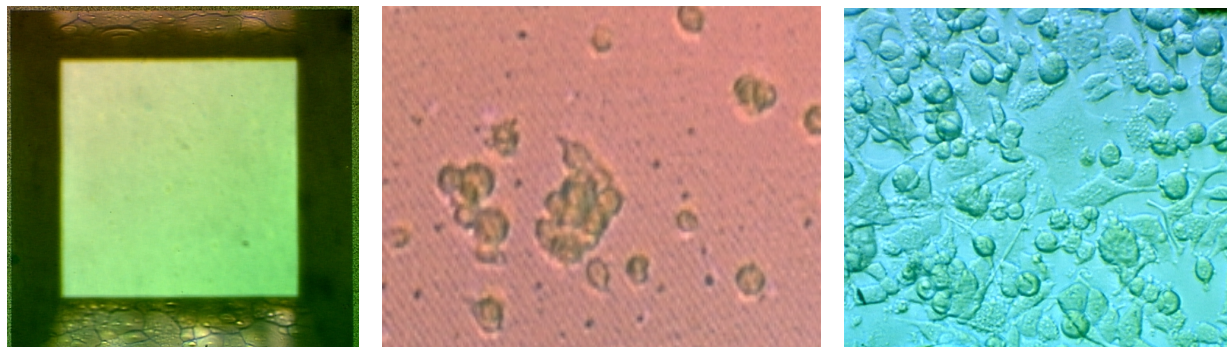


**Figure 8.** a) Empty nanoporous membrane and membrane seeded with PC12 cells seeded at b) day 1 and c) day 7. Cells show proliferation and differentiation within the nanoporous wells.

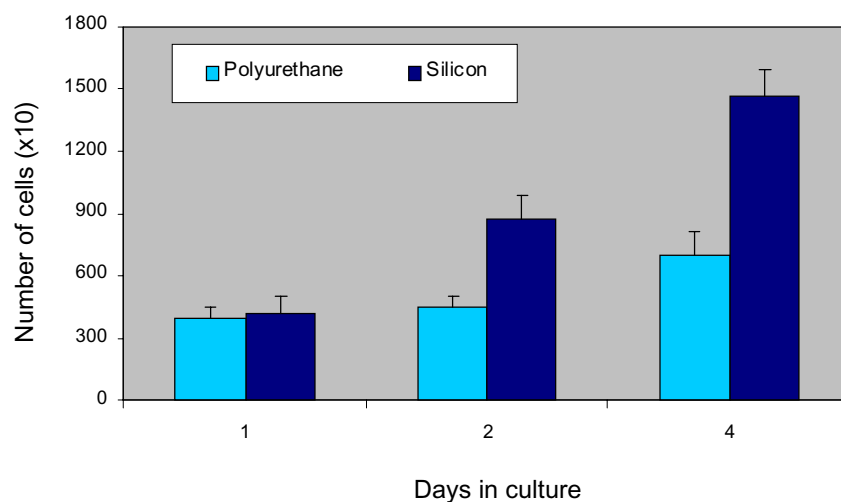


**Figure 9.** PC12 proliferation data in polyurethane (control) and silicon based capsules. Reported are average values of experiments performed with 3x standard deviations.

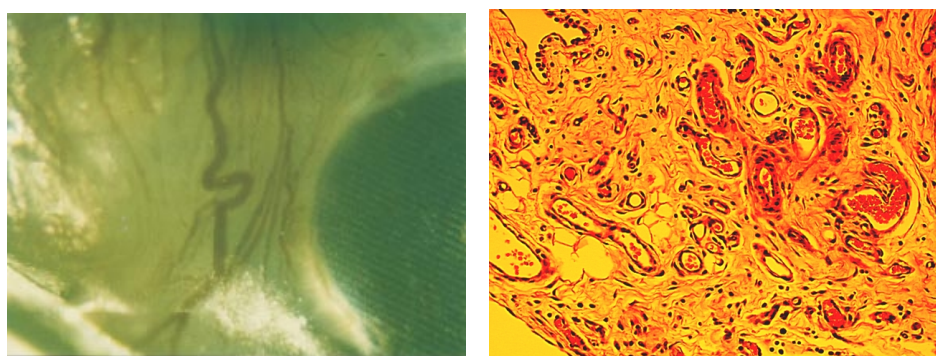


**Figure 10.** a) Nanoporous membrane retrieved from the peritoneal cavity: detail; b) H-E stained tissue (x20). Several blood vessels are visible (arrow).

### *In vivo Biocompatibility*

At a gross examination, silicon nanoporous membranes seemed free of fibrotic tissue and clean. A rich network of blood vessels surrounded the microfabricated membrane in proximity of the diffusion area, minimizing possible limitations of glucose-insulin exchange due to the lack of a well developed vascular system surrounding the membrane (figure 10a). Microscopic analysis of tissue sampled from the membrane located in the omentum revealed a non-uniform structure, with prevalence of large round cells typical of adipose tissue (figure 10b). There was no evidence of macrophages or lymphocytes infiltration. Round structures of different diameters resembling ducts could be seen. Their lumen presented secretion of probable proteinaceous origin. Adenomers were also dispersed in the tissue, as well as small vessels characterized by a thin layer of elongated cells, typical of the lining endothelium in capillaries.

### **Conclusion**

A method to create precise nanoporous membranes via microfabrication technology has been described. Membranes can be fabricated to present uniform and well-controlled pore sizes as small as 7 nm, tailored surface chemistries, and precise microarchitecture. These platforms can be interfaced with living cells to allow for biomolecular separation and immunoisolation. Ideally a membrane in contact with cells should be biocompatible and allow for the free exchange of nutrients, waste products, and secreted therapeutic proteins. Furthermore, where nutrients and time sensitive compounds are diffusing across a membrane it is highly desirable to be able to control the diffusion characteristic precisely in order to retain the dynamic response of seeded cells to external stimuli. Membranes were shown to be sufficiently permeable to support the viability of insulinoma and PC12 cells. Applications of these nanoporous membranes range from cellular delivery to cell-based biosensing to in vitro cell-based assays (figure 11).

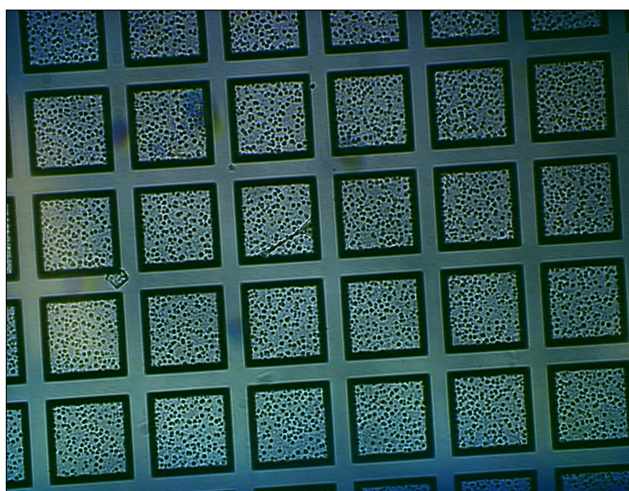


**Figure 11.** Arrays of nanoporous wells seeded with cell clusters that can potentially be used for high throughput cell-based assays.

In order to retain the same performance *in-vivo*, the biohybrid device must be fully biocompatible, which implies that the membrane should elicit little or no foreign body response. The host response is a potentially serious problem to clinical implementation of the technology. The direct consequence of a nonbiocompatible membrane is a fibrotic overgrowth on the surface that interferes with diffusive transport of molecules and oxygenated blood supply. The microfabricated nanoporous membrane proved to be highly biocompatible. After 2 week implantation into rat peritoneal cavity, there was no or minimal fibrotic tissue, no significant host response was elicited, and a rich microvascular system was surrounding the device.

## Experimental

The nanoporous membranes are achieved by applying fabrication techniques originally developed for Micro Electro Mechanical Systems (MEMS). Utilizing bulk and surface micromachining and microfabrication, silicon platforms can be engineered to have uniform and well-controlled pore sizes, channel lengths, and surface properties [8- 12]. We have developed several variants of microfabricated diffusion barriers, containing pores with uniform dimensions as small as 7 nanometers [10]. One such variation is described below.

### *Fabrication*

The process flow for fabrication of nanoporous membranes is depicted in Figure 1 below. The starting substrate is a 400  $\mu\text{m}$ -thick, 100 mm-diameter, double side polished (100)-oriented silicon wafer. The first step is the etching of the support ridge structure into the substrate. A low stress silicon nitride layer (nitride), which functions as an etch-stop, is then deposited. A polysilicon film, that acts as the base structural layer (base layer) is deposited on top of the etch-stop layer (Fig. 1a). The next step is the etching of holes in the base layer, which defines the overall shape of the pores. The holes are etched through the polysilicon by chlorine plasma, with a thermally grown oxide layer used as a mask. After the pore holes are defined and etched through the base layer (Fig. 1b), the pore sacrificial oxide is grown on the base layer (Fig. 1c). The sacrificial oxide thickness determines the pore size in the final membrane, so control of this step is critical to reproducible pores in the membrane.

To mechanically connect the base polysilicon with the plug polysilicon, which necessary to maintain the pore spacing between layers, anchor points are defined in the sacrificial oxide layer (Fig. 1d). After the anchor points are etched through the sacrificial oxide, the plug polysilicon is deposited to fill in the holes. The plug layer is then planarized down to the base layer (Fig. 1e), leaving the final structure with the plug layer only in the base layer openings. A protective nitride layer is then deposited on the wafer, completely covering both sides of the wafer (Fig. 1f). This layer is completely impervious to KOH chemical etch used to release the membranes from the bulk silicon wafer in the desired areas, and the wafer is placed at 80°C KOH bath to etch. After the silicon is completely removed up to the membrane, the protective, sacrificial, and etch stop layers are removed by etching in HF (Fig. 1g). The pores fabricated on the membranes were characterized by SEM. The nanoporous

membranes were seeded with islet cells, insulinoma cells, or PC12 cells and characterized in terms of viability, hormone secretion and/ proliferation.

#### *Insulinoma Cells*

Mouse insulinoma  $\beta$ TC3 cells (Efrat et al., 1998) have been obtained from the laboratory of Dr. Shimon Efrat, Department of Molecular Pharmacology, Albert Einstein College of Medicine, Bronx, NY. Cells are cultivated as monolayers in T-flasks in complete medium consisting of DMEM with 25 mM glucose and supplemented with 15% heat-inactivated horse serum (SIGMA) and 2.5% fetal bovine serum (SIGMA). Cultures are maintained at 37°C in a humidified 5% CO<sub>2</sub> /95% air atmosphere, and they are passed every 5-10 days. These cells maintain a stable phenotype of glucose responsiveness in the physiological range.

The membrane biocompatibility was characterized by direct contact tests looking at viability of cells in contact with silicon nanoporous membranes. The intracellular fluorescent dye carboxyfluorescein diacetate succinimidyl ester (CFDA, Molecular Probe) at a concentration of 5  $\mu$ M was used to label cells before in vitro culture. First cells were incubated in prewarmed CFDA labeling solution at 37 degrees C in a % CO<sub>2</sub> containing incubator for 45 minutes. The labeling solution was subsequently replaced by prewarmed DMEM medium supplemented with 10% FBS. Then, 10 $\mu$ l of 2x10<sup>7</sup> cells/ml were pipetted onto the membrane well. Cell viability was checked after 24 hours by counting with a hemacytometer under a light microscope. The viability was compared with cells grown on latex (negative control) and standard culture dishes. Cell attachment and proliferation to the various surfaces was also observed and measured.

#### *Neurosecretory Cells (PC12)*

PC12 cells (ATCC, Manassass, VA) of passages 3 to 5 were plated and at a density of 1-2 x 10<sup>6</sup> cells per 100 mm dish, maintained at 37 degrees C in 5% CO<sub>2</sub> and re-fed every 2-3 days. To determine the interaction between PC12 cells and silicon nanoporous membranes, the growth patterns of PC12 cells seeded at approximately 3-4 x10<sup>3</sup> cells into micromachined membrane-based biocapsules and polyurethane (control) capsules (n=3) contained in 12 well culture dishes were monitored at days 1, 2, and 4. After the designated incubation times, the silicon and control capsules were transferred to empty culture wells and rinsed with PBS to remove loosely adherent cells. Samples were then incubated with 1x trypsin-EDTA solution to detach the adherent cells. Cell suspensions were then centrifuged at 850 rpm for five minutes. PC12 cell pellets were resuspended in fresh DMEM media and counted twice with a hemocytometer. PC12 viability was monitored by labeling with intracellular fluorescent dye as described above.

#### *In-vivo Biocompatibility*

Implantation of nanoporous membranes were done according to the NIH guidelines for the care and use of laboratory animals. Male Lewis rats were anesthetized with inhalation of ether. A laparatomic incision was made and the biocapsules were either sutured on the abdominal wall or wrapped into the

omentum and sutured to the same. Incision was closed by suture (polypropylene). Capsules were retrieved after two weeks. Tissue samples were fixed in 10% buffered formalin, paraffin embedded, sectioned and stained with Hematoxylin-Eosin.

### Acknowledgements

Portions of this project were funded by NSF and The Whitaker Foundation. Special thanks to iMEDD, Inc. for technical support and fabrication of the membranes.

### References and Notes

1. Baxter, G.T.; Bousse, L.J.; Dawes, T.D.; Libby, J.M.; Modlin, D.N.; Owick, J.C.; Parce, J.W. *Clinical Chemistry* **1994**, *40*(9), 1800-1804.
2. Akin, T.; Najafi, K. *IEEE Transactions on Biomedical Engineering* **1994**, *4*(4), 305-313.
3. Volkmuth, W.D.; Duke, T.; Austin, R.H.; Cox, E.C. Trapping of branched DNA in microfabricated structures. *Proc. Natl. Acad. Sci. USA* **1995**, *92*(15), 6887-6891.
4. Gourley, P.L. *Nature Medicine* **1996**, *2*(8), 942-944.
5. Anderson, D.J.; Najafi, K.; Tanghe, S.J.; Evans, D.A.; Levy, K.L.; Hetre, J.F.; Xue, X.; Zappia, J.J.; Wise, K.D. *IEEE Transactions on Biomedical Engineering* **1989**, *36*(7), 693-704.
6. Santini, J.T. Jr.; Cima, M.J.; Langer, R. *Nature (London)* **1999**, 335-338.
7. Henry, S.; McAllister, D.V.; Allen, M.G.; Prausnitz, M.R. *J. Pharm. Sci.* **1998**, 922-925.
8. Desai, T.A.; Hansford, D.; Ferrari, M. *J. Membr. Sci.* **1999**, 221-231.
9. Desai, T.A.; Chu, W.H.; Tu, J.K.; Beattie, G.M.; Hayek, A.; Ferrari, M. *Biotechnol. Bioeng.* **1998**, 118-120.
10. Leoni, L.; Desai, T.A. Nanoporous Biocapsules for the Encapsulation of Insulinoma Cells: Biotransport and Biocompatibility Considerations. *IEEE Transactions in Biomedical Engineering*, Vol. 48 (11), November **2001**.
11. Desai, T. A.; Hansford, D. J.; Leoni, L.; Essenpreis, M.; Ferrari, M. Nanoporous Anti-fouling Silicon Membranes for Implantable Biosensor Applications. *Biosensors and Bioelectronics* **2000**, *15*(9-10), 453-462.
12. Desai, T.A.; Hansford, D.J.; Kulinsky, L.; Nashat, A.H.; Rasi, G.; Tu, J.; Wang, Y.; Zhang, M.; Ferrari, M. *Biomed. Microdevices.* **1999**, 11-40.

*Sample Availability:* Available from the authors.